

# Implementation of performance-based hybrid force/displacement seismic design in a building with steel frames

Bruno Ibáñez, Juan Carlos Vielma Pérez

Pontificia Universidad Católica de Valparaíso, Chile

**Abstract:** The Hybrid Force-Displacement (HFD) method combines the advantages of both seismic designs by applying a performance-based design approach, starting with a deformation design using these input variables. The maximum floor drifts and maximum roof displacements that exceed the elastic limit of the sections are controlled using three performance levels. Each of these levels is represented by an elastic acceleration spectrum and another elastic displacement spectrum, which are used to perform the seismic force design. The procedure involves modifying the spectrum, scaling its ordinates, and thus obtaining a representation of the three performance levels. The maximum roof responses for each performance level are thus obtained, and the respective reduction or behavior factors are then calculated. To illustrate the application of the method, a 7-story building structured with moment-resistant steel frames, located in a high seismic demand zone such as Valparaíso, Chile, was studied. The procedure is validated by applying nonlinear dynamic time history analysis using records of strong earthquakes occurring in the subduction zone.

**Key words:** hybrid force-displacement method; moment frame buildings; maximum roof displacement; mezzanine drifts

## 1. Introduction

The provisions of the Chilean Seismic Standard Nch433 [1] basically define the design seismic action, which depends on the seismic zone, type of foundation soil, occupancy category and the type of earthquake-resistant system used in its structuring, establishing two analysis methods, the equivalent static and the spectral modal [2]. In addition, this regulation limits the relative floor displacements and torsional effects, requiring for this an inelastic spectrum of both acceleration and displacement. On the other hand, the AISC 360 code [3] establishes the procedures for the verification and design of steel structural elements (beams and columns) for combined loads according to the applied regulations, in this case Nch1537 [4]. The usual design implies that the beams will be verified in bending and shear, independently, while the columns will be calculated for the interaction of bending and axial force (flexural-compression) [5, 6].

On the other hand, performance-based seismic design consists of the selection of appropriate assessment schemes that allow the sizing and detailing of structural, non-structural and contained components, so that, for certain ground motion levels and with certain reliability levels, damage to the structures should not exceed certain limit states [7, 8]. A performance level represents a limiting or tolerable condition established based on three fundamental aspects [9, 10]:

- Possible physical damage to structural and non-structural components
- Threat to the safety of the building's occupants, induced by these damages

- Functionality of the building after the earthquake

Therefore, according to the background indicated above, it is observed that the Chilean seismic regulations mainly carry out a design by forces, in which through spectral modal analysis the seismic shear forces of design are obtained, and to evaluate the displacements they use limits of interstory drifts.

The hybrid force-displacement design (HFD) [11] on which this document focuses, combines the advantages of seismic force design and seismic displacement design. This method begins by considering target deformations (displacement target) for both structural and non-structural elements, in terms of maximum story drifts and local ductility of the members, thus obtaining roof displacements as a function of both initial variables, in addition to the reduction factor  $q$ . The application of the method continues with a seismic force design, focusing on the verification of the applied forces, using for this the pseudo-acceleration design spectrum analysis for the determination of seismic forces.

The direct displacement design method is the most widely used among those existing worldwide [12], it is based on the fact that the original inelastic structure consisting of a multiple degrees of freedom (MDOF) system is replaced by an equivalent linear single degree of freedom (SDOF) structure with a modified amount of damping. Using this equivalent structure (SDOF) in conjunction with a design displacement spectrum with a large amount of damping, the seismic base shear forces required for the structure to experience the desired deformation in the form of the target story drift ratio (IDR) can be determined. Structural and non-structural damage are controlled by imposing limits only on story drifts (IDR).

## 2 Methodology

This section explains the basic steps for using the hybrid force-displacement (HFD) method applied to a case study involving a steel moment frame structure and a collaborating slab, located in a highly seismic zone in the Valparaíso region of Chile, considering torsional effects and accidental eccentricities. The explicit empirical expressions required by the method, involving deformation transformations and the reduction factor ( $q$ ), are determined by means of a nonlinear time history (NLTH) analysis.

### 2.1 Characteristics and properties of the model

The following eight steps explain the application of the hybrid design method [11].

Step 1. The geometric characteristics of the frame are defined, including the number of floors ( $n_s$ ), number of spans ( $n_b$ ), floor height ( $h$ ) and span lengths ( $b$ ), both in the horizontal and vertical directions respectively, in its plan view.

Step 2. The performance levels considered are defined with seismic intensity levels provided by the corresponding elastic response spectra:

- Immediate Occupancy
- Life Safety
- Collapse Prevention

Step 3. The maximum story drift (IDR) and maximum local ductility of the member  $u_0$  are defined as in the displacement-based method (DBD) in terms of performance input (Target).

Table 1 gives these limits for the three performance levels indicated above [11]. The local ductility values represent the slenderness limits of the flanges and web and the axial force limits of the columns. The values in parentheses comply with ASCE 41 [13].

Table 1. Input values for both story drift and local ductility for each performance level

Immediate Occupancy (IO)		Life Safety		Collapse Prevention	
IDR	$u_0$	IDR	$u_0$	IDR	$u_0$
0.007	1.00	0.025	9.00	0.05	1.00

Source: [11]

Step 4. One of the ways to estimate the roof yielding displacement ( $u(r,y)$ ) is through nonlinear dynamic analysis, in which the following formula was proposed [11]:

$$u_{r,y} = 0,034 \cdot n_s^{0,61} \cdot \rho^{0,075} \cdot \alpha^{-0,254} \quad (1)$$

Where:

$n_s$  is the number of floors

$\rho$  is the ratio of the moment of inertia ( $I_b$ ) to the length of beams ( $L_b$ ) and the inertia ( $I_c$ ) to the length of columns ( $L_c$ ), respectively, determined by expression 2:

$$\rho = \left( \frac{\sum \left( \frac{I_c}{L_c} \right)}{\sum \left( \frac{I_b}{L_b} \right)} \right) \quad (2)$$

$\alpha$  relationship between the plastic moments of resistance of the columns ( $M_{Rc,1av}$ ) and the plastic moments of the beams ( $M_{Rb,av}$ ) of all floors, determined by the expression 3

$$\alpha = \left( \frac{M_{Rc,1av}}{M_{Rb,av}} \right) \quad (3)$$

The values of parameters  $b_1$  and  $b_2$  are then presented, which depend on the number of floors, the structure to be analyzed, and the input values that the story drifts (IDR) will have for each performance level. These parameters will subsequently be used to transform maximum target story drifts (Target) into target roof displacements (Target). Where  $b_1$  and  $b_2$  are parameters dependent on the number of floors ( $n_s$ ) and the level of maximum displacement (IDR),  $H$  is the total height of the building expressed in meters (see Table 2).

Table 2. Values of parameters  $b_1$  and  $b_2$  as a function of the number of floors and IDR above the yield strength limit

Number of Stories $n_s$	IDR <sub>y</sub> –IDR1.8%		IDR1.8%–IDR3.2%		IDR>IDR3.2%	
	$b_1$	$b_2$	$b_1$	$b_2$	$b_1$	$b_2$
3	0.84	1.01	1.03	1.06	0.99	1.05
6	0.37	0.88	0.93	1.11	1.51	1.25
9	0.29	0.88	2.07	1.37	2.38	1.41
12	0.28	0.91	1.46	1.32	5.58	1.71
15	0.22	0.89	5.04	1.67	6.88	1.76

Step 5. Transformation of the maximum floor drift IDR (Target) to the maximum roof displacement  $u_{r,max}$  (Objective), determined by expression 4, and for the transformation of the maximum  $u_0$  (Objective) to the maximum roof displacement (Objective) expression 5:

$$u_{r,max}(IDR) = b_1 \cdot H \cdot (IDR^{b_2}) \quad (4)$$

$$u_{r,max}(u_0) = (u_{r,o}) \cdot (u_{r,y}) \quad (5)$$

$u_{r,0}$  being the maximum roof rotational ductility in terms of local ductility, determined by:

$$u_{r,0} = 1 + 0,85 \cdot (u_o - 1) \quad (6)$$

$$u_{r,0} = 2,58 + 0,38 \cdot (u_o - 1) \quad (7)$$

Therefore, the maximum design roof displacement is obtained through expression 8:

$$u_{r,max}(d) = \min(u_{r,max}(IDR), u_{r,max}(u_o)) \quad (8)$$

Step 6. In addition, the reduction factor ( $q$ ) of the structure is calculated:

$$q = 1 + 1,35 \cdot (u_{r,d} - 1) \quad (9)$$

Disregarding accidental eccentricity

$$q = 1 + 1,3 \cdot (u_{r,d} - 1) \quad (10)$$

Considering accidental eccentricity

where  $u_{r,d}$  is the design roof displacement ductility, expressed as:

$$u_{r,d} = u_{r,max} / u_{r,y} \quad (11)$$

Step 7. Design the structure by the Force Method using elastic response spectral analysis, based on an elastic spectrum with the ordinates divided by the reduction factor ( $q$ ) as in the force-based method.

It is observed from Figure 1 that  $u(r,max)$  is the maximum displacement obtained by the displacement spectra according to the performance level IO, LS and CP respectively, that for this document the displacement spectrum of NCh433 will be used. If  $u(r,max)$  is less than  $u(r,max)(d)$ , as shown in Figure 1.

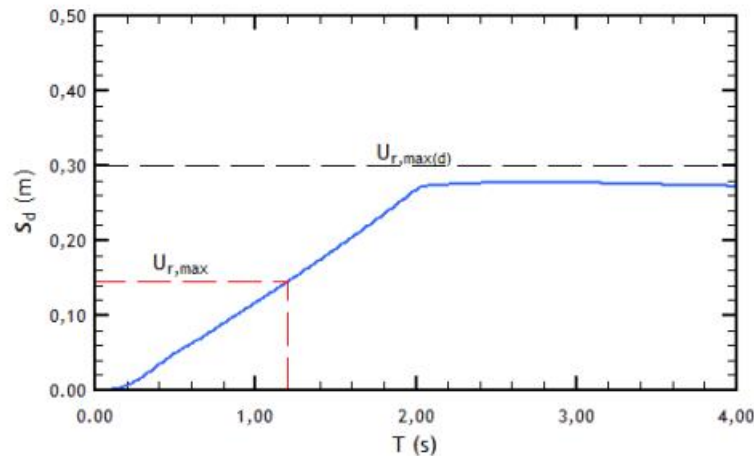


Figure 1. Determination of  $u(r,max)$  using the elastic displacement design spectrum

Source: adapted from [11]

A new target value (Target) of maximum roof design displacement is adopted as the value obtained by  $u_{(r,max)}$  and the method continues smoothly.

Based on the new value  $u_{(r,max)}(d)$ , the new target values corresponding to  $IDR_{max}$  and  $u_{(r,max)}$  can be calculated again with the design equations.

Step 8. Finally, to obtain the roof displacement (expression 12) of a multi-degree-of-freedom (MDOF) structure more accurately, the spectral displacement of the structure in one degree of freedom (SDOF) obtained above must be multiplied

by a modification factor equal to 1.0, 1.2, 1.3, 1.4 and 1.5 for buildings with 1, 2, 3, 5 and greater than or equal to 10 floors respectively.

$$\text{Roof displacement} = 1.42 \cdot u_{r,max} \quad (12)$$

## 2.2 Case study

The case study corresponds to a building with special moment-resistant steel frames, without bracing, in the Valparaíso region, Chile, which corresponds to seismic zone 3, soil type C and occupancy category type II, and also has the following geometric characteristics:

- Number of floors Import image 7
- Floor height (h) 3.00 m
- Material: A36 structural steel
- Distance between spans (b) 5.00 m
- HEB550 Columns Section
- Main Beams Section IPE400, IPE450
- Secondary Beams Section IPE 240

The building is considered to be made of moment-resistant steel frames, with a total height of 21 m, a floor height of 3 m each, and a distance between spans of 5 m each, as indicated above, and the geometric characteristics are shown in Figures 2 and 3. The structure is assumed to have an accidental eccentricity of 5%. The steel grade is assumed to be A36 for both beams and columns, respectively. In addition, the first level is assumed to be Immediate Occupancy (IO) under the Full Operational Earthquake (FOE), the second level is assumed to be Life Safety (LS) under the Design Basis Earthquake (DBE), and the third level is assumed to be Collapse Prevention (CP) under the Maximum Considered Earthquake (MCE), for a 50-year exceedance probability of 2%, corresponding to the maximum seismic hazard level, with a return period of 2,500 years.

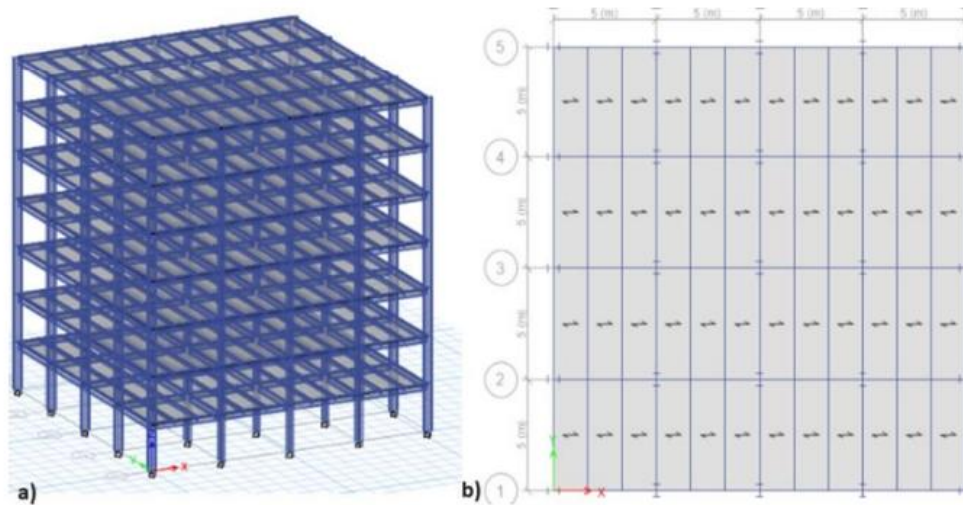


Figure 2. (a) 3D view and (b) plan view of the building studied

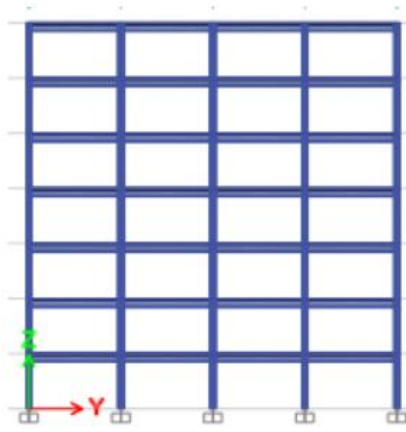


Figure 3. Elevation view of the building studied

Source: the authors

The characteristic earthquakes FOE, DBE and MCE are expressed through the elastic design spectrum of Nch433, for soil type C, seismic zone 3, and maximum ground acceleration  $A_0$  under DBE equal to  $0.4g$  as shown in Figure 4. The maximum ground acceleration  $A_0$  under FOE and MCE is obtained:

$$PGA_{FOE} = 0,3 * PGA_{DBE} = 0,3 \cdot 0,4 \cdot g \quad (13)$$

$$PGA_{MCE} = 1,5 * PGA_{DBE} = 1,5 \cdot 0,4 \cdot g \quad (14)$$

It can be observed from Figures 4 and 5 that the acceleration and displacement spectrum of the Nch433 corresponds to the second LS performance level under the DBE. For the first performance level IO under the FOE, there is 30% of the maximum ground acceleration ( $A_0$ ) of the second LS performance level under the DBE. For the third performance level CP under the MCE, there is 1.5 times the maximum ground acceleration of the second LS performance level under the DBE. For this project, a value of  $u_{r,y} = 0.086$  m defined in [11] is obtained, because it is based on many nonlinear dynamic analyses. In addition, it provides greater precision in the result because the variable  $\rho$  represents the influence of the elastic response, and the variable  $a$  represents the influence of the inelastic response. In addition, this last factor has a greater influence on the results.

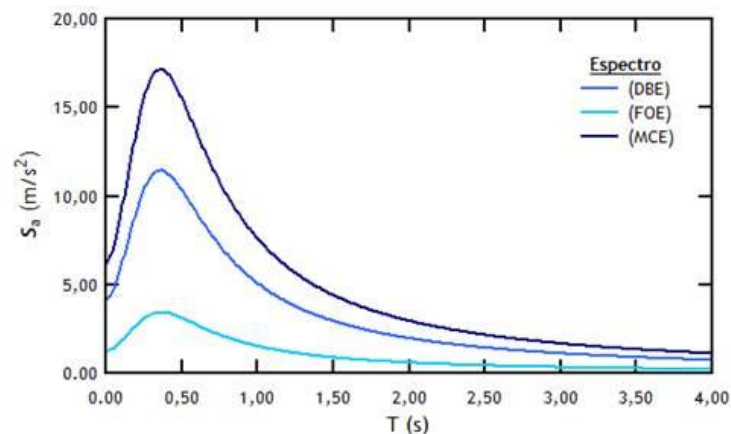


Figure 4. Acceleration spectra for each performance level

Source: the authors

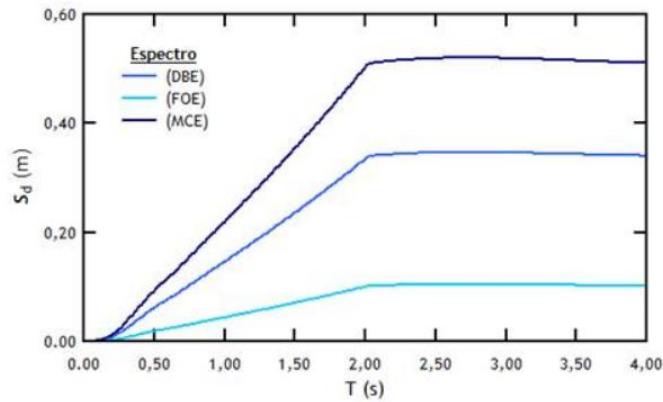


Figure 5. Acceleration spectra for each performance level

Source: the authors

For the purposes of this study, parameters  $b_1$  and  $b_2$  were used corresponding to the number of floors equal to 7, therefore, through a linear interpolation, said parameters are obtained as represented in Table 3.

Table 3. Values of parameters  $b_1$  and  $b_2$  as a function of the number of floors and IDR above the yield strength limit

	$b_1$	$b_2$
IO: IDR 0.7%:	0.343	0.880
LS: IDR 2.5%:	1.310	1.197
CP: IDR 5%:	1.800	1.303

Source: the authors

Therefore, for this project, which consists of a 7-story building, a value of 1.42 is obtained by interpolating the above data. By performing the procedure explained above, Table 4 lists the maximum inter-story drifts, maximum roof displacements, and maximum local ductilities for both the x and y directions, as well as according to the IO, LS, and CP performance levels, respectively.

Table 4. Maximum inter-story drifts obtained from the HFD method

Direction	Immediate occupancy (IO)	Life safety (LS)	Collapse prevention (CP)
X	0.0048	0.0180	0.0264
Y	0.0036	0.0140	0.0215

Source: the authors

On the other hand, Tables 5 and 6 show the results obtained for the maximum roof displacements and the ductilities calculated for the different limit states of this study.

Table 5. Maximum inter-story drifts obtained from the HFD method

Direction	Immediate occupancy (IO)	Life safety (LS)	Collapse prevention (CP)
X	0.006	0.224	0.332
Y	0.051	0.169	0.0254

Source: The authors

Table 6. Maximum inter-story drifts obtained from the HFD method

Direction	Immediate occupancy (IO)	Life safety (LS)	Collapse prevention (CP)
X	1.000	3.000	4.500
Y	1.000	2.200	3.400

Source: The authors

After calculating the maximum story drifts, maximum roof displacements and local ductilities for each performance level, a nonlinear time-history (NLTH) analysis is performed to verify the methods obtained by the HFD Method. For the purposes of the time-history dynamic analysis, the acceleration records [14] that cover the earthquakes in the localities of

Valparaiso, Coquimbo, and Puerto Quellón, which have been entered into the SeismoStruct program [15], are considered. In addition, scaling factors were used for each record to represent the performance level, immediate occupancy (IO), life safety (LS), and collapse prevention (CP). The main characteristics of the seismic records used in this study are summarized in Table 7.

Table 7. Accelerogram records used for nonlinear time history analysis

Earthquake	Station	Identification	Maximum Acceleration (m/s <sup>2</sup> )
Valparaiso	Las Torpederas	Valparaiso_Torpederas_EW_SD	0.56213
	Las Torpederas	Valparaiso_Torpederas_NS_SD	0.4747
Coquimbo	El Pedregal	Coquimbo_El_Pedregal_EW_SD	0.51606
	El Pedregal	Coquimbo_El_Pedregal_NS_SD	0.49965
Puerto Quellón	Loncomilla	Puerto_Quellon_Loncomilla_EW-SD	0.40257
	Loncomilla	Puerto_Quellon_Loncomilla_NS-SD	0.46458
Coquimbo	San Esteban	Coquimbo_Tololo_EW_SD	0.49813
	San Esteban	Coquimbo_Tololo_NS_SD	0.46454
Puerto Quellón	Hotel Luna	Coquimbo_San_Esteban_EW_SD	0.5021
	Hotel Luna	Coquimbo_San_Esteban_EW_SD	0.46621
Coquimbo	Tololo	Puerto_Quellon_HotelLuna_EW_SD	0.43542
	Tololo	Puerto_Quellon_HotelLuna_NS_SD	0.45233

Source: The authors

Regarding Figure 6, it can be observed that the building is being subjected to accelerations at the base, both in the x and y directions respectively (green color) and is also subjected to the loads that are exerted on the beams (blue color) corresponding to the dead load of the structure and the live load.

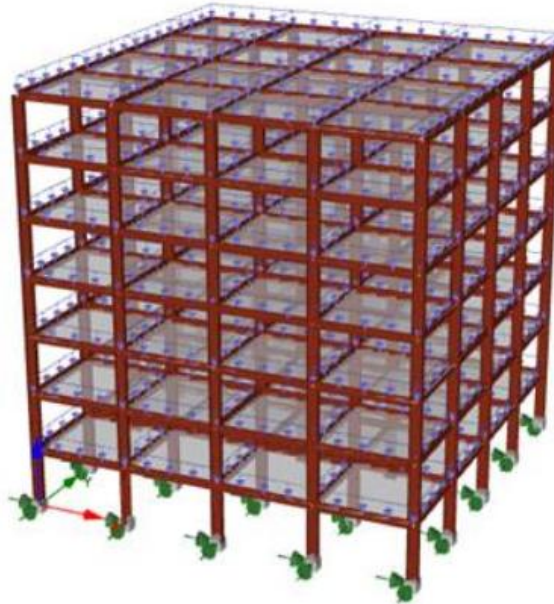


Figure 6. Building model in SeismoStruct

Source: the authors

### 3 Results and discussion

The results obtained from the nonlinear time history (NLTH) analysis using SeismoStruct software are compared with the results obtained from the Hybrid Force-Displacement (HFD) method presented in this paper. The results of the comparison are shown in Tables 8 and 9, for the X and Y directions of the building, respectively.

Table 8. IDR,  $u_{r,max}$  and  $u_0$  obtained by both HFD and NLTH in the x direction

Hybrid force-displacement method HFD						
Direction X	IO under FOE		LS under DBE		CP under MCE	
	FHD	NLTH	FHD	NLTH	FHD	NLTH
IDR %	0.500	0.480	2.400	1.800	2.700	2.640
$u_{r,max}$	0.066	0.050	0.224	0.212	0.332	0.334
$u_0$	1.000	1.100	3.000	3.000	4.500	4.500

Source: the authors

Table 9. IDR,  $u_{r,max}$ , and  $u_0$  obtained by both HFD and NLTH in the y direction

Hybrid force-displacement method HFD						
Direction Y	IO under FOE		LS under DBE		CP under MCE	
	FHD	NLTH	FHD	NLTH	FHD	NLTH
IDR %	0.480	0.360	1.400	1.400	2.150	2.150
$u_{r,max}$	0.051	0.046	0.169	0.169	0.254	0.233
$u_0$	1.000	1.000	2.200	2.100	3.400	3.400

Source: the authors

Therefore, looking at Tables 8 and 9, it can be seen that the Hybrid Force-Displacement Design (HFD) method presents values that resemble the results obtained by a nonlinear analysis, thus demonstrating the closeness of the calculations. That is, there is a good approximation in the estimation of the maximum roof displacement for each performance level, which allows for the design of moment-resistant steel frame buildings with roof displacements as input variables, imposing a deformation load on the structure. Furthermore, it is important to mention that, when selecting the sections of both beams and columns, they will impose a roof yielding displacement determined by the geometric characteristics of the building, and it is this displacement that will be used for the first performance level as the maximum roof displacement. Likewise, as a result of these analyses, the base sections corresponding to the three performance levels IO, LS, and CP are obtained, considering the factors 0.3; 1.0 and 1.5, respectively.

Table 10 shows the basal cuts generated in the building, considering the three performance levels, so it can be observed that the basal cuts in scale 0.3 correspond to the elastic cut in the building, which presents ductility 1 indicated in Table 6, that is, the elastic cut corresponds to the design cut for that case, which means that the quotient between elastic basal cut and design basal cut have values very close to those obtained in ductility indicated in Table 6.

Table 10. Baseline cuts calculated for different scale factors

Base Shear $V_e$ (kN)			
Record	Scale 0.3	Scale 1.0	Scale 1.5
1	2,600	9,070	13,010
2	2,380	7,960	11,930
3	1,860	6,210	9,320
4	2,300	7,680	11,520
5	2,320	7,740	11,610
6	2,010	6,710	10,070
Average ( $V_e$ )	2,250	7,560	11,240
Maximum $V_e$	2,600	9,070	13,010
Minimum $V_e$	1,860	6,210	9,320

Source: the authors

Considering the application of the HFD method for this 7-story building, it can be observed that the sections indicated in Table 11 were used.

Table 11. Structural design sections

Section	Columns	Beams		
	HEB550	Direction X	Direction Y	Secondary
		IPE400	IPE450	IPE240

Source: the authors

These sections allow the building to respond to the deformation demands requested of it, exceeding the plasticization deformation, that is, they are sections that allow the building to enter the inelastic range, which allows this Hybrid Force Displacement Method to be applied optimally. In addition, it can be observed that the Method estimates maximum roof displacements that are close to the inelastic displacements represented by the structure, because this method uses the deformations as input variables in the design, which leads to a more accurate result. In addition, it can be observed from the results that this Method allows obtaining reduction factors for each performance level, based on the displacements, unlike the current Chilean Seismic regulation NCh433 that uses a reduction factor ( $R^*$ ) that is a function of other parameters, such as the oscillation period of the structure and the soil, which allows obtaining safe values regarding the ductility that the building will present in the face of a seismic event.

#### 4 Conclusions

First, it should be noted that when a seismic event occurs, structures deform, and these deformations induce internal stresses. This means that the input variables that generate earthquakes are deformations. Therefore, introducing a method that considers these variables for design ensures optimal nonlinear behavior in structures, which in turn allows for the design of safer structures. Furthermore, this hybrid method allows for identifying the performance level that controls the design and provides accurate predictions of rotational ductility and roof displacement.

On the other hand, it allows to obtain the inelastic deformation that said structure will present, which unlike the Method used by the current Chilean regulation Nch433 does not allow damage to the elements, and said damage allows energy to be dissipated, so that, if the Method is carried out correctly, it will allow resources to be optimized so that they can dissipate maximum energy and respond to the seismic events that are generated. On the other hand, this alternative seismic design presents an interesting implementation proposal in earthquake-resistant designs in Chile, since, although structural steel has a higher economic cost, it can be useful for design alternatives in buildings in Chile, so for low or medium-rise buildings they present an effective and innovative solution.

#### Conflicts of interest

The author declares no conflicts of interest regarding the publication of this paper.

#### References

- [1] Norma Chilena, "*NCh433.Of1996-Modificado 2012. Diseño Sísmico de Edificios*", INN, Santiago, Chile, 2012.
- [2] R. Riddell y P. Hidalgo, "*Diseño Estructural*", Ediciones UC, Santiago, Chile, 2018
- [3] AISC, "Specification for Structural Steel Buildings. AISC 360", American Institute of Steel Construction, Chicago, Estados Unidos de América, 2022
- [4] NCh1537 Of86, "*Diseño Estructural de Edificios – Cargas Permanentes y Sobrecargas de uso*", INN, Santiago, Chile, 1986
- [5] J. C. Vielma, "Evaluación de la vulnerabilidad sísmica de estructuras de acero residenciales del Ecuador", *Monografía CIMNE IS 70, Monografías de ingeniería sísmica*, Barcelona, España, ISBN: 978-84-941686-9-7, 2015
- [6] J. C. Vielma y M. Cando, "Influence of P-delta effect on ductility of SMRF steel buildings" *The Open Civil Engineering Journal*, V9, 351-359, <https://doi.org/10.2174/1874149501509010351>, 2015

- [7] G. Papagiannopoulos, G. Hatzigeorgiou y D. Beskos, "*Seismic Design Methods for Steel Building*", Springer, Heidelberg, Alemania, 2022
- [8] Federal Emergency Management Agency and the National Institute of Building Sciences, "*FEMA273*", 1997
- [9] J. C. Vielma y M. Cando, "Evaluación del factor de comportamiento de la Norma Ecuatoriana de la Construcción para estructuras metálicas porticadas", *Revista Internacional de Métodos Numéricos para cálculo y diseño en Ingeniería*, 33, 271-279, 2017
- [10] N. Lisperguier, A. López, y J. C. Vielma, "Seismic performance assessment of a moment-resisting frame steel warehouse provided with overhead crane", *Materials*, 16, 2815, <https://doi.org/10.3390/ma16072815>, 2023
- [11] I.A. Dimououlos, N. Bazeos y D.E. Beskos, "Seismic Yield Displacements of Plane moment resisting and x-braced Steel Frames", *Soil Dynamics and Earthquake Engineering*, 140, pp. 121-144, <https://doi.org/10.1016/j.soildyn.2012.05.002>, 2012
- [12] M.J.N. Priestley, G.M. Calvi y M.J. Kowalsky, "*Displacement-Based Seismic Design of Structures*" IUSS Press, Pavia, Italia, 2008
- [13] American Society of Civil Engineer, ASCE/SEI, 41-17, "*Seismic evaluation and retrofit of existing buildings*", ASCE standard, Estados Unidos, 2013
- [14] Consortium of Organizations for Strong-Motion Observation Systems (COSMOS), "*Virtual Data Center*", Disponible en: <https://www.strongmotioncenter.org/vdc/scripts/default.plx>, 2017
- [15] Seismosoft Ltd., "*SeismoStruct 2021 User Manual - A computer program for static and dynamic nonlinear analysis of framed structures*", Disponible en: <https://seismosoft.com/>, 2021

#### **Author's Notes**

1. Bruno Ibáñez. Civil Engineer. Pontifical Catholic University of Valparaíso. Email: [bruno.ibanez.d@mail.pucv.cl](mailto:bruno.ibanez.d@mail.pucv.cl)
2. Juan Carlos Vielma Pérez. Civil Engineer. Master of Science in Structural Engineering, University of Los Andes, Venezuela. PhD from the Polytechnic University of Catalonia, Spain. Research Professor at the Pontifical Catholic University of Valparaíso, Chile. Email: [juan.vielma@pucv.cl](mailto:juan.vielma@pucv.cl)